Journal of Advances in Mathematics and Computer Science

Volume 40, Issue 8, Page 155-169, 2025; Article no.JAMCS.142217
ISSN: 2456-9968
(Past name: British Journal of Mathematics & Computer Science, Past ISSN: 2231-0851)

Impact of an Inclined Magnetic Field on Thermo-concentration Boundary Layers in Unsteady Micropolar Magnetohydrodynamic Flow over a Nonlinear Stretching Sheet

R.A. Mutegi [a*], M.O. Okongo [a] and J. Ochwach [b]

[a] Department of Physical Sciences, Chuka University, P.O. Box 109-60400, Chuka, Kenya.
[b] Department of Computing and Information Technology. Mama Ngina University College, Gatundu, Kenya.

Authors' contributions

This work was carried out in collaboration among all authors. All authors read and approved the final manuscript.

Article Information

DOI: https://doi.org/10.9734/jamcs/2025/v40i82037

Open Peer Review History:
This journal follows the Advanced Open Peer Review policy. Identity of the Reviewers, Editor(s) and additional Reviewers, peer review comments, different versions of the manuscript, comments of the editors, etc are available here: https://pr.sdiarticle5.com/review-history/142217

Original Research Article

Received: 10/06/2025
Published: 16/08/2025

Abstract

This work investigates the influence of an inclined magnetic field on thermo-concentration boundary layers in a micropolar magnetohydrodynamic (MHD) fluid flow over a nonlinear stretching surface. The magnetic field is applied at an inclination angle, altering the Lorentz force and hence affecting flow, heat, and mass transfer characteristics. Similarity transformations reduce the governing partial differential equations to ordinary differential form, which are further converted to a set of first-order ordinary differential equations and solved

**Corresponding author: Email: alexmutegirwanda@gmail.com;*

Cite as: *Mutegi, R.A., M.O. Okongo, and J. Ochwach. 2025. "Impact of an Inclined Magnetic Field on Thermo-Concentration Boundary Layers in Unsteady Micropolar Magnetohydrodynamic Flow over a Nonlinear Stretching Sheet". Journal of Advances in Mathematics and Computer Science 40 (8):155-69. https://doi.org/10.9734/jamcs/2025/v40i82037.*

numerically using a collocation method in MATLAB. The results, which describe the impact of varying the angle of inclination of the magnetic field on the fluid velocity, angular velocity, temperature, concentration, skin friction, Nusselt number, and Sherwood number of the micropolar fluid, are presented in graphical and tabular form. They show that a 62.5% increase in the angle of inclination α ,increases the fluid velocity by 17.1% and temperature profile by 8.4% while the particle's angular velocity and concentration decreases by 13.4% and 7.1% respectively and that a 29.2 % rise in the unsteadiness parameter lowers the fluid velocity by 3.3% and improves the angular velocity and temperature by 5.1% and 16.7% respectively. Further, the skin friction coefficient and Nusselt number increase with an increase in the angle of the inclination but Sherwood number decreases. For a higher unsteadiness parameter, the Nusselt number and Sherwood number increases but the skin friction decreases. The findings have significant implications for the design and control of MHD-based thermal systems where the orientation of the magnetic field and time dependent flow behavior plays a crucial control role for optimum performance. The results are consistent with existing literature on magnetic field orientation in unsteady fluid flow systems.

Keywords: Inclined magnetic field; micropolar fluid Lorentz force; skin friction; Nusselt number; Sherwood number; stretching sheet.

1 Introduction

Inclined magnetic fields are increasingly used in industrial magnetohydrodynamic (MHD) applications such as cooling systems, plasma technology, and electromagnetic separation. In micropolar fluids, the orientation of the magnetic field alters the interaction between microstructure rotation and fluid convection. Existing studies have largely focused on vertically applied magnetic fields or neglected micropolar effects altogether, especially under unsteady and nonlinear stretching conditions. This study addresses this gap by investigating how varying the inclination angle α influences fluid viscosity, heat and mass transfer via the skin friction, Nusselt and Sherwood numbers. The concept presents a more realistic and broader model of MHD flows in engineering systems such as plasma devices, MHD generators, and nuclear reactor cooling. The incorporation of micropolar fluid behavior captures microstructural aspects significant in biological fluids and liquid crystals, while the nonlinear stretching and unsteady flow reflect practical conditions in materials processing, extrusion, and polymer manufacture.

A numerical study of natural convection of a nanofluid in an inclined L-shaped cavity in the presence of an inclined magnetic field was done by (Elshehabey et al., 2014), where the emphasize was to identify the symmetrical behavior in fluid motion and temperature distribution at specific magnetic field angles. Srivastava, (2014) conducted a study on the flow characteristics of blood via an inclined tapered porous artery with minor stenosis under an inclined magnetic field. Raju et al., (2015) examined how radiation, an angled magnetic field, and cross-diffusion affect flow over a stretching surface. The study found that aligning the angle strengthens the magnetic field, reducing fluid flow, friction factor, and mass transfer rate while boosting heat transmission inside the fluid. Heat transfer and inclined magnetic field analysis for peristaltically driven motion of tiny particles was investigated by (Bhatti et al., 2017), while (Mutegi et al., 2021) investigated how an angled magnetic field affects magnetohydrodynamic (MHD) boundary layer flow on a porous exponentially stretched sheet exposed to thermal radiation. Srinivasulu & Goud, (2021) investigated how an angled magnetic field affects flow, heat, and mass transfer of Williamson nanofluids across a stretching sheet. Vijayalakshmi & Sivaraj, (2023) analyzed heat transfer on micropolar alumina-silica-water nanofluid flow in an inclined square cavity with inclined magnetic field and radiation efficiency. Irreversibility of micropolar nanofluid flow in a vertical channel under the influence of an angled magnetic field and a heat source or sink was investigated by (Shobha & Patil, 2022) while (Mahabaleshwar et al., 2024) studied the effects of a ternary nanofluid on a micropolar fluid with angled MHD, slip flow, and heat transfer. The main focus here was to establish how the orientation of the magnetic field affects fluid flow and thermal characteristics. Elmhedy et al., (2024) studied the effect of an inclined magnetic field and heat transfer on peristaltic flow of the Rabinowitsch fluid model in an inclined channel whereby the observation was that the magnetic field inclination act as a controlling mechanism for peristaltic flow. Dar & Elangovan, (2017) investigated the impact of an inclined magnetic field, heat generation/absorption, and radiation on the peristaltic flow of a micropolar fluid through a porous non-uniform channel with slip velocity, while Dar, (2021) studied the peristaltic motion of micropolar fluid with slip velocity in a tapered asymmetric channel in the

presence of an inclined magnetic field and thermal radiation. Heat and mass transfer on free convective flow of a micropolar fluid through a porous surface with an inclined magnetic field and Hall effects was investigated by (Krishna et al., 2019), where the main focus was to examine how an inclined magnetic field together with the Hall current affects the heat and mass transfer of the micropolar fluid. (Umadevi et al., 2021) analyzed the impact of an inclined magnetic field on non-isothermal vertical surface flow of micropolar fluid embedded in porous stratum. The inclined magnetic field and thermal radiation effect on electroosmotic flow of a micropolar fluid through a porous microchannel was investigated by (Dar & Elangovan, 2017), where the main focus of the study was on electroosmotic propulsion in microfluidic channels. (Pop et al., 2023) investigated the unsteady flow and heat transfer of nanofluids, hybrid nanofluids, micropolar fluids and porous media, and (Reddy & Anki Reddy, 2021) carried out a numerical simulations of unsteady 3D MHD micropolar fluid flow over a slendering sheet, where the study underscored that the microstructural dynamics plays a critical role in the shaping of the microrotation characteristics of the micropolar fluid. Heat transfer in unsteady separated stagnation point flow of a micro-polar fluid was examined by (Sadiq et al., 2022). To extend on this concept (Fatunmbi et al., 2023) investigated the Entropy generation analysis in an unsteady hydromagnetic micropolar fluid flow along an exponentially stretchable sheet with slip properties. Walelign, (2025) analyzed the Casson nanofluid transport rates near a vertical stretching sheet with dissipation and slip effects and Walelign, (2024) studied the rates of heat, mass and momentum transfer in a magnetic nanofluid near cylindrical surface with velocity slip and convective heat transfer. Based on the literature above, the angle of inclination of the magnetic field has a considerable influence on the flow, temperature, and concentration properties of micropolar MHD flows across nonlinear stretching sheets. It impacts velocity profiles, heat transmission, and boundary layer thicknesses, all of which are important in a variety of industrial applications. Therefore, this area has not been fully explored; hence, understanding it well enables better control and optimization of micropolar fluid-based operations.

2 Mathematical Formulation

2.1 Description of the problem

In this study, unsteady and, incompressible micropolar fluid flow over a nonlinearly stretching sheet subjected to an inclined magnetic field is considered. The flow analysis is performed in a two-dimensional Cartesian coordinate system, with the x-axis aligned with the stretching surface at y=0 and the y-axis perpendicular to it, as shown in Fig. 1. The fluid moves with the velocity $u_w = \frac{ax^n}{1-\gamma t}$, where n > 1 represents the nonlinearity parameter and γ signifies unsteadiness. The transverse magnetic field $\vec{B}(x,t) = \frac{\overrightarrow{B_0} x^{\frac{n-1}{2}}}{(1-\gamma t)^{\frac{1}{2}}}$ is applied at an angle α with the y axis. The magnetic component introduces a modified Lorentz force proportional to $-\sigma u B^2 \cos^2\alpha + \sigma v B^2 \sin\alpha\cos\alpha + \sigma v H B \cos\alpha$.

The stretched sheet's temperature $T_w = T_\infty + \frac{ax^{2n-1}}{(1-\gamma t)^2}$, is controlled by a heated fluid behind the wall, with a convective temperature and a constant wall concentration $C_w = C_\infty + \frac{ax^{2n-1}}{(1-\gamma t)^2}$. The free stream conditions are represented by T_∞ and C_∞, which reflect the ambient temperature and concentration respectively.

2.2 Governing Equations

The flow is governed by continuity, momentum, Angular momentum, Energy and Concentration equations as described by (Patel et al., 2022). These equations are as shown:

Continuity equation;

$$\frac{\partial u}{\partial x}+\frac{\partial v}{\partial y}=0\ \cdot \tag{1}$$

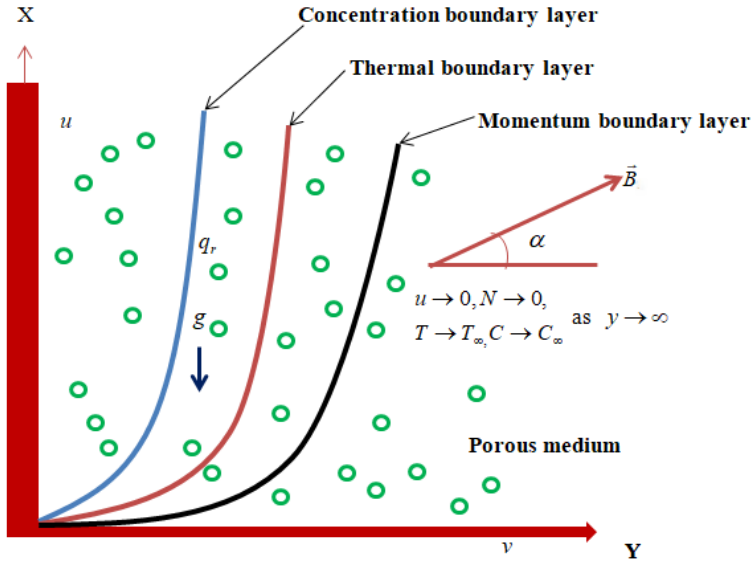

Fig. 1. Sketch of the physical problem

Momentum equation;

$$\frac{\partial u}{\partial t}+u\frac{\partial u}{\partial x}+v\frac{\partial u}{\partial y}=-\frac{\mu}{\rho k'}u+\frac{\mu+\kappa}{\rho}\frac{\partial^2 u}{\partial y^2}+\frac{\kappa}{\rho}\frac{\partial N}{\partial y}+\frac{\sigma v B^2\sin\alpha\cos\alpha-\sigma u B^2\cos^2\alpha+\sigma v H B\cos\alpha}{\rho}$$
$$+g\beta_T(T-T_\infty)+g\beta_C(C-C_\infty). \tag{2}$$

Angular momentum equation;

$$\frac{\partial N}{\partial t}+\left(u\frac{\partial N}{\partial x}+v\frac{\partial N}{\partial y}\right)=\left(\frac{\gamma_v}{\rho j}\right)\frac{\partial^2 N}{\partial y^2}-\left(\frac{\kappa}{\rho j}\right)\left(2N+\frac{\partial u}{\partial y}\right)\cdot \tag{3}$$

Energy equation;

$$\frac{\partial T}{\partial t}+u\frac{\partial T}{\partial x}+v\frac{\partial T}{\partial y}=\frac{k_2}{\rho C_p}\frac{\partial^2 T}{\partial y^2}+\frac{\mu+\kappa}{\rho C_p}\left(\frac{\partial u}{\partial y}\right)^2+\frac{\sigma(uB\cos\alpha-v(B\sin\alpha+H))^2}{\rho C_p}+\frac{16\sigma^*}{3k^*\rho C_p}T_\infty^3\frac{\partial^2 T}{\partial y^2}$$
$$+\left(\frac{k_2 u(x,t)}{xv\rho C_p}\right)[A^*(T_W-T_\infty)f'+B^*(T-T_\infty)]. \tag{4}$$

And Concentration equation.

$$\frac{\partial C}{\partial t}+u\frac{\partial C}{\partial x}+v\frac{\partial C}{\partial y}=D\frac{\partial^2 C}{\partial y^2}+\frac{D_T}{T_\infty}\frac{\partial^2 T}{\partial y^2}-k_2(C-C_\infty)\cdot \tag{5}$$

The boundary equations are:

$$u = u_w, \quad v = 0, \quad N = -m_0 \frac{\partial u}{\partial y}, \quad -k_2 \frac{\partial T}{\partial y} = h_f (T_w - T), \quad C = C_w, \quad \text{as} \quad y \to 0. \tag{6}$$

And

$$u \to 0, \quad N \to 0, \quad T \to T_\infty, \quad \text{and} \quad C \to C_\infty \quad \text{as} \quad y \to \infty \tag{7}$$

2.3 Similarity transformation

Using similarity variables,

$$\begin{aligned} &\eta = \sqrt{\frac{a(n+1)}{2\nu(1-\gamma t)}} x^{\frac{n-1}{2}} y, \quad N = \frac{ax^n}{1-\gamma t} \sqrt{\frac{a(n+1)}{2\nu(1-\gamma t)}} x^{\frac{n-1}{2}} g(\eta), \\ &u = \frac{ax^n}{1-\gamma t} f'(\eta), v = -\sqrt{\frac{a\nu(n+1)}{2(1-\gamma t)}} x^{\frac{n-1}{2}} \left[f(\eta) + \frac{n-1}{n+1} \eta f'(\eta) \right], \\ &\theta(\eta) = \frac{T - T_\infty}{T_w - T_\infty}, \quad \phi(\eta) = \frac{C - C_\infty}{C_w - C_\infty}, \quad H = \frac{B_0 x^{\frac{n-1}{2}}}{(1-\gamma t)^{\frac{1}{2}}} h'(\eta) \end{aligned} \tag{8}$$

The governing PDEs are transformed as:

Momentum;

$$\begin{aligned} &(1+K) f''' + f f'' - \frac{2n}{n+1} f'^2 - \frac{\tau}{n+1} (2 f' + \eta f'') + \frac{2}{n+1} (\lambda_T \theta + \lambda_C \phi) - \frac{2}{n+1} k_1 - M \Big(\frac{2}{n+1} f' \cos^2 \alpha \\ &+ \frac{1}{2} Re^{-\frac{1}{2}} f \sin 2\alpha + \frac{n-1}{2(n+1)} Re^{-\frac{1}{2}} \eta f' \sin 2\alpha + Re^{-\frac{1}{2}} f h' \cos \alpha + \frac{n-1}{n+1} Re^{-\frac{1}{2}} \eta f h' \cos \alpha \Big) + K g' = 0 \end{aligned} \tag{9}$$

Angular momentum;

$$\left(1 + \frac{K}{2}\right) g'' + f g' - \frac{\tau}{n+1} (3g + \eta g') - \left(\frac{3n-1}{n+1} \right) g f' - \frac{2K}{n+1} (2g + f'') = 0 \tag{10}$$

Energy equation;

$$\begin{aligned} &2Pr\tau\theta + \frac{Pr\tau}{2} \eta\theta' + Pr(2n-1)\theta f' - Pr(\frac{n+1}{2}) f\theta' = \frac{(n+1)}{2} \theta'' + Pr\,Ec(1+K)(\frac{n+1}{2}) f''^2 \\ &+ Pr\,EcM[f'^2 \cos^2 \alpha + Re^{-1}(\frac{(n+1)^2}{4} f^2 + \frac{(n^2-1)}{2} \eta f f' + \frac{(n-1)^2}{4} \eta^2 f'^2) \sin^2 \alpha + Re^{-1}(\frac{(n+1)^2}{4} f^2 h'^2 \\ &+ \frac{(n^2-1)}{2} \eta f f' h'^2 + \frac{(n-1)^2}{4} \eta^2 f'^2 h'^2) + Re^{-\frac{1}{2}}(\frac{(n+1)}{2} f f' + \frac{(n-1)}{2} \eta f'^2) \sin 2\alpha + \\ &Re^{-\frac{1}{2}}((n+1) f f' h' + (n-1)\eta f'^2 h') \cos \alpha + Re^{-1}(\frac{(n+1)^2}{2} f^2 h' + (n^2-1)\eta f f' h' + \frac{(n-1)^2}{2} \eta^2 f'^2 h') \sin \alpha] + \\ &\frac{4}{3} Nr \left(\frac{n+1}{2} \right) \theta'' + A^* f' + B^* \theta \end{aligned} \tag{11}$$

And concentration equation.

$$\phi'' + Sc\left(f\phi' - \frac{4n-2}{n+1}\phi f' \right) - \frac{2Sc\tau}{n+1}\left(2\phi + \frac{1}{2}\eta\phi' \right) + \frac{N_t}{N_b}\theta'' - \frac{2}{n+1}K_r\phi = 0 \tag{12}$$

Key dimensionless parameters in the resulting equations above are; the unsteadiness parameter, $(\tau = \frac{\gamma x}{ax^n})$, the permeability parameter $(k_1 = \frac{\nu x}{ak_0})$, the micropolar parameter $(K = \frac{\kappa}{\mu})$, the magnetic parameter $(M = \frac{\sigma B_0^2}{a\rho})$, the Grashof number based on temperature differences $(Gr = \frac{g\beta_T\theta(T_w - T_\infty)x^3}{\nu^2})$, the Reynolds number $(Re = \frac{u_w x(n+1)}{2\nu})$,the temperature mixed convection parameter $(\lambda_T = \frac{Gr}{Re^2})$, the Grashof number for mass transfer $(Gr_m = \frac{g\beta_C\phi(C_w - C_\infty)x^3}{\nu^2})$, Concentration mixed convection parameter $(\lambda_C = \frac{Gr_m}{Re^2})$, the Prandtl number $(Pr = \frac{\mu C_p}{k_2})$, the Eckert number $(Ec = \frac{u_w^2}{C_p(T_w - T_\infty)})$, Thermal radiation $(N_r = \frac{4\sigma * T_\infty^3}{k * k_2})$, Schmidt number $(Sc = \frac{\nu}{D})$, chemical reaction parameter $(K_r = k_2\frac{(1-\gamma t)x}{ax^n})$,Brownian parameter, $(N_b = \frac{\rho C)_\rho D(C_w - C_\infty)}{\nu(\rho C)_f})$ and Thermophoresis parameter $(N_t = \frac{(\rho C)_\rho D_T(T_w - T_\infty}{\nu(\rho C)_f})$

The non-dimensionalised boundary conditions are given as below;

$$f'(\eta) = 1,\ f(\eta) = 0, g(\eta) = -m_0 f''(\eta), \theta'(\eta) = -Bi\left(1 - \theta(\eta)\right), \phi(\eta) = 1 \text{ as } \eta \to 0 \tag{13}$$

$$f'(\eta) \to 0, g(\eta) \to 0, \theta(\eta) \to 0, \phi(\eta) \to 0 \text{ as } \eta \to \infty \tag{14}$$

3 Numerical Method

3.1 Conversion of a higher order odes to a system of first order odes

To solve the resulting ODEs numerically, they are first converted into a system of first order odes as below:

Let $f = y_1, f' = y_2, f'' = y_3, g = y_4, g' = y_5, \theta = y_6, \theta' = y_7, \phi = y_8, \phi' = y_9, h = y_{10}$ and $h' = y_{11}$

So that;

$$y'_1 = y_2,$$

$$y'_2 = y_3,$$

$$y'_3 = -\frac{1}{1+K}\Big[y_1 y_3 - \frac{2n}{n+1}y_2^2 - \frac{\tau}{n+1}\left(2y_2 + \eta y_3\right) + \frac{2}{n+1}\left(\lambda_T y_6 + \lambda_C y_8 - k_1\right)$$
$$-M\Big(\frac{2}{n+1}y_2\cos^2\alpha + \frac{1}{2}Re^{-\frac{1}{2}}y_1\sin 2\alpha + \frac{n-1}{2(n+1)}Re^{-\frac{1}{2}}\eta y_2\sin 2\alpha + Re^{-\frac{1}{2}}y_1 y_{11}\cos\alpha +,$$
$$\frac{n-1}{n+1}Re^{-\frac{1}{2}}\eta y_2 y_{11}\cos\alpha\Big) + Ky_5\Big]$$
$$y'_4 = y_5,$$

$$y'_5 = -\frac{1}{1+\frac{K}{2}}\left[y_1 y_5 - \frac{\tau}{n+1}\left(3y_4 + \eta y_5\right) - \left(\frac{3n-1}{n+1}\right) y_2 y_4 - \frac{2K}{n+1}\left(2y_4 + y_3\right)\right],$$

$$y'_6 = y_7,$$

(15)

$$y'_7 = \frac{1}{1+\frac{4}{3}Nr}\left[\frac{2Pr\tau}{n+1}\left(2y_6 + \frac{1}{2}\eta y_7\right) + Pr\left(\frac{2n-1}{n+1}\right) y_2 y_6 - Pr\,Ec(1+K) y_3^2\right.$$

$$-Pr\,EcM\left(\frac{2}{n+1} y_2^2 \cos^2\alpha + Re^{-1}\left[\frac{n+1}{2} y_1^2 + (n-1)\eta y_1 y_2 + \frac{(n-1)^2}{2(n+1)}\eta^2 y_2^2\right]\sin^2\alpha + \right.$$

$$Re^{-1}\left[\frac{n+1}{2} y_1^2 y_{11}^2 + (n-1)\eta y_1 y_2 y_{11}^2 + \frac{(n-1)^2}{2(n+1)}\eta^2 y_2^2 y_{11}^2\right] + Re^{-\frac{1}{2}}\left[y_1 y_2 + \frac{n-1}{n+1}\eta_2^2\right]\sin 2\alpha +$$

$$Re^{-\frac{1}{2}}\left[2y_1 y_2 y_{11} + \frac{2(n-1)}{n+1}\eta y_2^2 y_{11}\right]\cos\alpha + Re^{-1}\left[(n+1) y_1^2 y_{11} + (n-1)\eta y_1 y_2 y_{11} + \frac{(n-1)^2}{n+1}\eta^2 y_2^2 y_{11}\right]\sin\alpha\Big)$$

$$\left. - \frac{2}{n+1}(A^* y_2 + B^* y_6)\right],$$

$$y'_8 = y_9,$$

$$y'_9 = -Sc\left[y_1 y_9 - \frac{4n-2}{n+1} y_2 y_8\right] + \frac{2Sc\tau}{n+1}\left(2y_8 + \frac{1}{2}\eta y_9\right) - \frac{N_t}{N_b} y_{7'} + \frac{2}{n+1} K_r y_8,$$

$$y'_{10} = y_{11}.$$

The boundary conditions are;

$$y_2 = 1, y_1 = 0, y_4 = -m_0 y_3, y_7 = -Bi\left(1 - y_6\right), y_8 = 1 \text{ as } \eta \to 0 \tag{16}$$

$$y_2 \to 0, y_4 \to 0, y_6 \to 0, y_8 \to 0 \text{ as } \eta \to \infty \tag{17}$$

The physical quantities crucial to this study are the skin friction, Nusselt number and Sherwood number as described by the equations below.

skin friction,

$$Re^{\frac{1}{2}} C_f = \sqrt{\frac{n+1}{2}}(1 + (1-m_o)K) f''(0) \tag{18}$$

Nusselt number,

$$Re^{-\frac{1}{2}} Nu = -\sqrt{\frac{n+1}{2}}\theta'(0) \tag{19}$$

Sherwood number

$$Re^{-\frac{1}{2}}Sh = -\phi'(0) \tag{20}$$

3.2 Numerical solution

To solve the system of first-order equations obtained above, rewrite it in vector form as

$$\vec{y}' = g'(\eta, \vec{y}, \vec{p}) \ , \ 0 \le \eta < \infty \ . \tag{21}$$

where $\vec{P}$ is a vector of unknown parameters, $\vec{y} = (y_1, ..., y_{11})^T$ and $\vec{g} = (g_1, ..., g_{11})^T$. To simplify the solution, the boundary conditions are stated as $\vec{h}(\vec{y}(0), \vec{y}(\infty)) = 0$ after suppressing $\vec{P}$. The system is numerically solved using a collocation approach based on piecewise cubic polynomials over a discretized mesh $0 = \eta_0 < \eta_1 <, ... < \eta_N = \infty$. At the endpoints and midpoints of each subinterval, the approximate solution $\vec{S}(\eta)$ meets the system requirements. The results obtained is a nonlinear algebraic system that is solved repeatedly through linearization. To ensure accuracy, the residual is minimized using $|\vec{y}(\eta) - \vec{S}(\eta)| = Ch^4$. This method generates precise and computationally efficient approximations for velocity, temperature, angular velocity, and concentration profiles under a variety of parameters and their conditions. The angle α is varied from 0° to 90° to assess the impact on transport rates.

4 Results and Discussion

This section looks at how the magnetic field's angle of inclination affects the fluid flow's velocity, temperature, angular velocity, and concentration profiles. The findings are presented graphically, followed by a thorough discussion. Furthermore, the impact of the angle of inclination of the magnetic field on the skin friction, Nusselt number, and Sherwood number of the micropolar fluid is assessed.

4.1 Effects of angle of inclination of the magnetic feld (α)

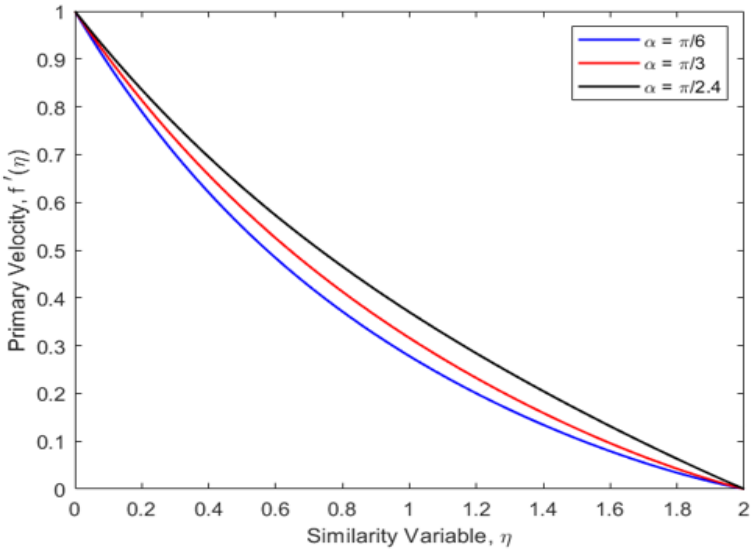

Fig. 2. Effect of the angle of inclination of the magnetic field on the velocity profile

Figs. 2-5 illustrates the effects of the angle of inclination of the magnetic field on the velocity, angular velocity, temperature, and concentration profiles of the micropolar fluid. A 62.5% increase in the angle of the inclination reduces the Lorentz force as the magnetic field aligns with the fluid flow. This lowers resistance and enhances fluid velocity, thereby improving the velocity profile by 17.1%, as shown by Fig. 2. The angular velocity of the micropolar fluid particles decreases by 13.4%, as depicted by Fig. 3. This is due to higher fluid velocity, which makes the particles become more resistant to rotation, leading to a decrease in the angular velocity. The overall temperature profile increases by 8.4%, as shown by Fig. 4**.** This improvement is due to enhanced convective heat transfer resulting from higher fluid velocity, which occurs when the Lorentz force is reduced. However, at a lower angle of inclination of the magnetic field, the temperature near the surface drops slightly due to a larger Lorentz force, which slows fluid motion, thereby reducing convective heat transmission. As a result, temperatures decrease more quickly near the surface. Fig. 5 shows that the concentration profile decreases by 7.1% due to reduced Lorentz force, which leads to a higher fluid velocity away from the surface. This improves the convective transport of fluid particles, resulting in a lower concentration profile. This concept is important to systems such as nuclear reactor cooling channels, plasma containment devices, polymer extrusion lines, and biofluidic devices, where the orientation of the magnetic field can be controlled to optimize fluid and heat transfers.

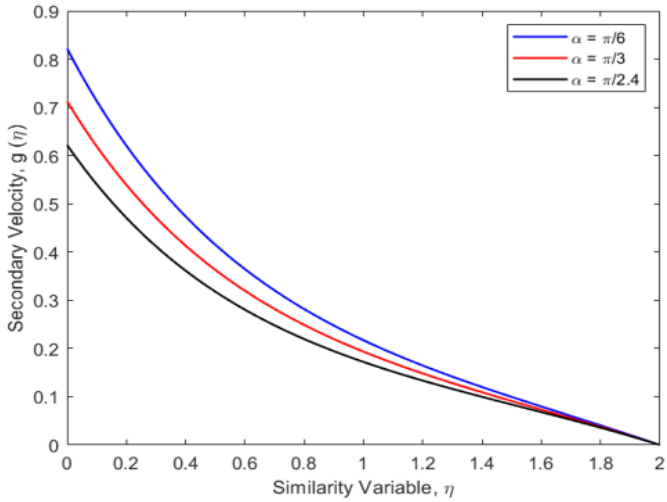

Fig. 3. Effect of the angle of inclination of the magnetic field on the angular velocity profile

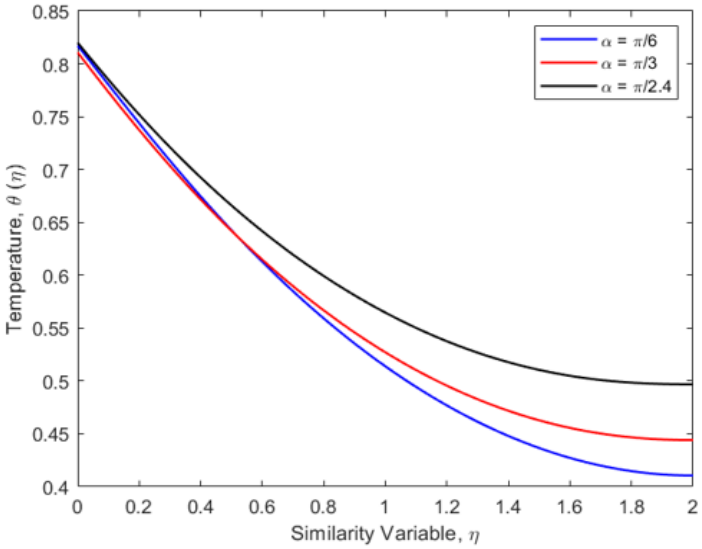

Fig. 4. Effect of the angle of inclination of the magnetic field on the temperature profile

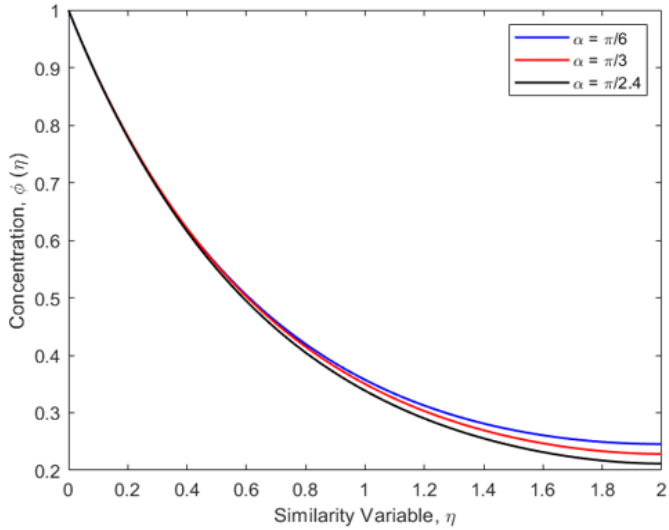

Fig. 5. Effect of the angle of inclination of the magnetic field on the concentration profile

4.2 Effects of unsteadiness parameter (τ)

Figs. 6-9 illustrate the effects of the unsteadiness parameter on the micropolar fluid properties. The results show that increasing the unsteadiness parameter by 29.2% decreases the fluid's velocity by 3.3%, as shown in Fig. 6. This is due to flow fluctuations and resistance caused by variation of the velocity fields over time. As a result, the momentum boundary layer lowers, reducing fluid velocity. The angular velocity increases by 5.1% near the surface, but this quickly dissipates and converges for higher η values as the fluid flows away from the surface, as illustrated by Fig. 7. This occurs due to reduction of particle momentum, which results in amplification of the rotational effects, increasing fluid angular velocity. The fluid temperature increases by 16.7%, as shown by Fig. 8. This is as a result of the reduction of the thermal boundary layer due to flow resistance, which enhances heat transmission between the surface and the fluid. The prolonged exposure of the fluid on the surface causes rapid heat loss to the surroundings, leading to a drop in fluid temperature. The concentration profile increases slightly, as in Fig. 9, since unsteady flow alters the velocity field over time, leading to increased mixing and diffusion of species. Higher transport rates cause more solute particles to disperse and accumulate away from the surface, increasing fluid concentration. The concept of unsteadiness in micropolar fluid is crucial in the engineering field as it is applied in devices such as biomedical, thermal systems and lubrication where time dependent flow behavior affects efficiency, performance and reliability.

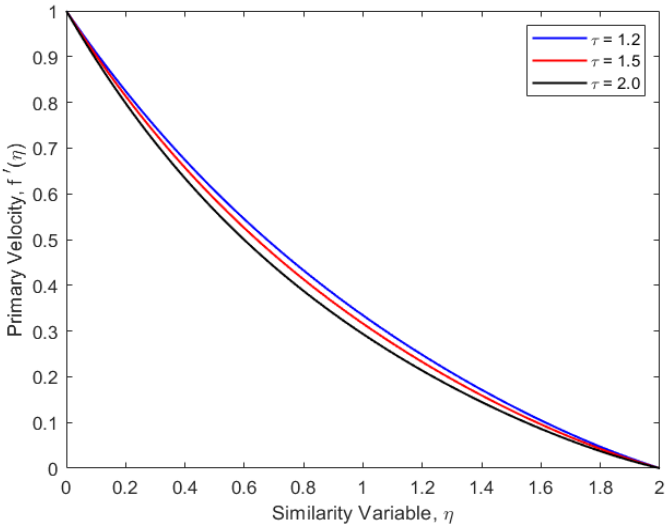

Fig. 6. Effect of unsteadiness parameter on the velocity profile

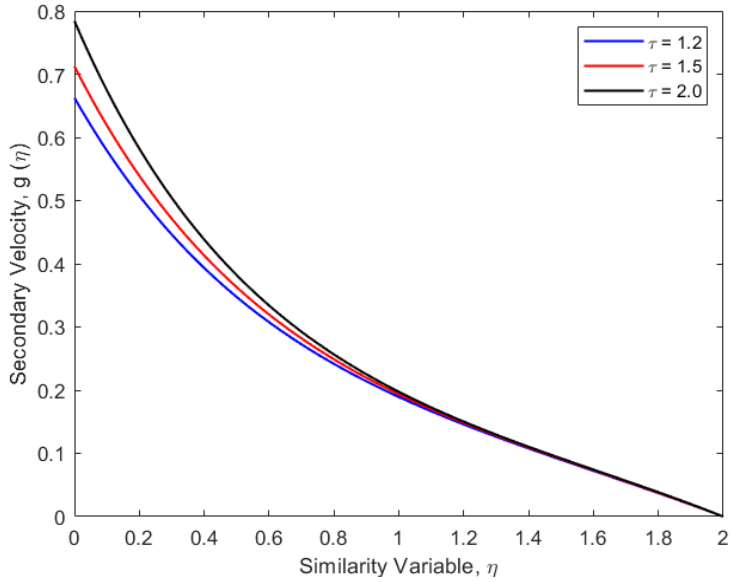

Fig. 7. Effect of unsteadiness parameter on the angular velocity profile

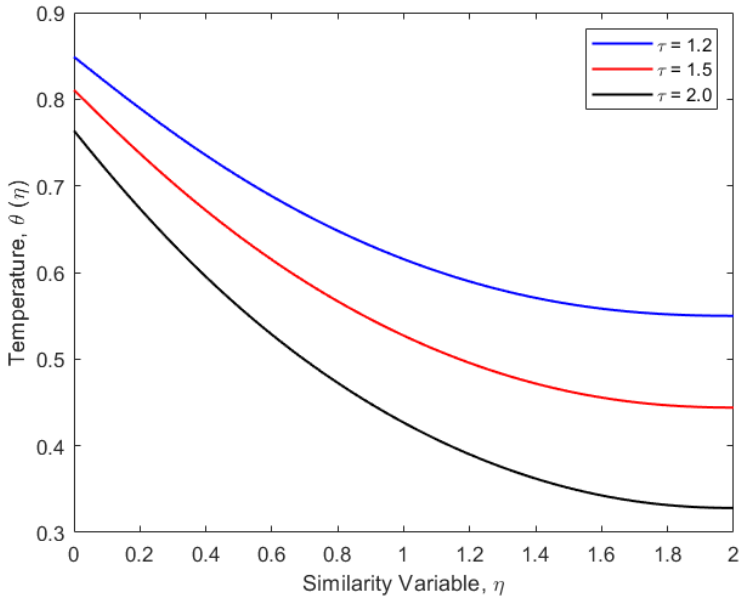

Fig. 8. Effect of unsteadiness parameter on the temperature profile

4.3 Effects of Angle of Inclination of the Magnetic Field on Skin Friction, Nusselt Number and Sherwood Number

Table 1 presents the effects of the angle of inclination and unsteadiness parameters on the skin friction, Nusselt number, and Sherwood number of the micropolar fluid. The results show that increasing the angle of inclination of the applied magnetic field causes an increase in skin friction. This occurs due to a decrease in Lorentz force as the magnetic field aligns with the flow direction. The reduced opposing force allows fluid to flow more easily, increasing its velocity near the wall. The velocity gradient near the wall increases, causing shear stress and increased skin friction. The Nusselt number increases as the applied magnetic field's angle of inclination increases. This is because the magnetic field aligns with the flow direction, making the Lorentz force decrease. This lowers the resistance to fluid flow, improving the convective heat transmission, which results in a thinner thermal boundary layer and stronger temperature gradients, increasing the Nusselt number. The Sherwood

number decreases with an increase in the angle of inclination of the applied magnetic field. This is due to the weakening of the Lorentz force, which reduces magnetic resistance to flow. This leads to increased fluid velocity and thicker velocity boundary layer at the surface, which enhance hydrodynamic resistance near the surface, slowing convective mass transfer and resulting in a lower Sherwood number.

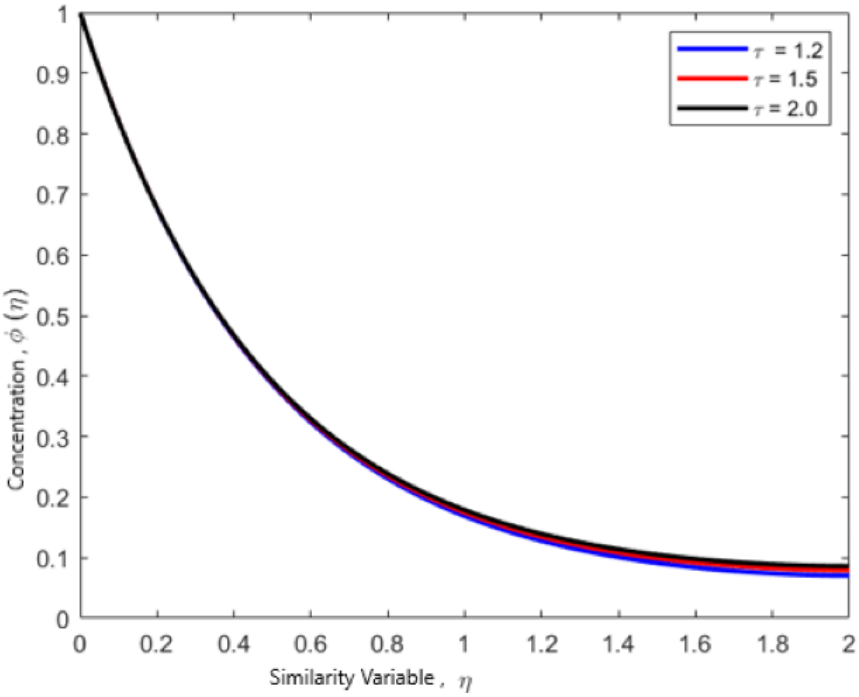

Fig. 9. Effect of unsteadiness parameter on the concentration profile

The increase in the unsteadiness parameter, which describes the flow's time-dependent nature, reduces skin friction. This is due to temporal changes in velocity and microrotation, reducing fluid momentum near the wall, which in turn lowers the velocity gradient at the wall, lowering shear stress and skin friction coefficient. Higher unsteadiness parameter values increase the Nusselt number, since unsteady flow causes increased variance in fluid velocity, which thins the thermal boundary layer, increasing the temperature gradient at the wall. Resulting in an increased heat transmission. The Sherwood number increases with the unsteadiness parameter due to variation in fluid velocity as a result of its time-dependent nature. Stronger velocity variations reduce the concentration boundary layer, increasing the gradient near the surface. The increased mass transfer from the surface to the fluid results in a greater Sherwood number.

Table 1. Numerical values of C_f , Nu and Sh for angle of inclination of the magnetic field

Parameter	**value**	C_f	Nu	Sh
Angle of inclination of magnetic field (α)	$\frac{\pi}{6}$	-1.8272	0.4501	1.2589
	$\frac{\pi}{3}$	-1.5920	0.4620	1.2425
	$\frac{5\pi}{12}$	-1.3921	0.4717	1.2407
Unsteadiness parameter (τ)	1.2	-1.4843	0.3701	1.2348
	1.5	-1.5920	0.4620	1.2425
	2.0	-1.7457	0.5743	1.2643

4.4 Validation with previous literature

To validate the results obtained above and confirm the correctness of the numerical method of solution, the computed values of the skin friction, Nusselt number and Sherwood number, were found to be in agreement with the results published by (Sheikh & Hasan, 2017). Similarly, the results for the same physical quantities with respect to the unsteadiness parameter, were in agreement with the findings of (Shamshuddin et al., 2019). This confirm that the present results are valid and scientifically reliable.

5 Conclusion

The Impact of Inclined Magnetic Field on Thermo-Concentration Boundary Layers in Unsteady Micropolar MHD Flow over a nonlinear stretching sheet was explored. The governing equations for continuity, momentum, angular momentum, energy, and concentration were developed and converted into higher-order ordinary differential equations via similarity transformations. The nonlinear equations were then transformed into a set of first-order ordinary differential equations. The resulting system was numerically solved by collocation method in MATLAB, and the results were presented graphically and in tabular form. The effects of the magnetic field's angle of inclination and unsteadiness parameter on the fluid velocity, angular velocity, temperature, and concentration profiles were investigated. Furthermore, numerical values of the skin friction coefficient, Nusselt number and Sherwood number were determined. The main conclusions are:

- The fluid velocity increases as the angle of inclination of the magnetic field increases, but decreases with increase in the unsteadiness parameter.
- The fluid temperature increases with increase in the angle of inclination of the magnetic field and the unsteadiness parameter.
- The angular velocity decreases with increase in the angle of inclination of the magnetic field but increases with increase in the unsteadiness parameter.
- The concentration profile decreases with increase in the angle of inclination of the magnetic field but increases slightly with increase in unsteadiness parameter.
- The skin friction coefficient increases with increase in the angle of inclination of the magnetic field but decreases with increase in unsteadiness parameter.
- The Nusselt number increases with increase in the angle of inclination of the magnetic field and the unsteadiness parameter.
- The Sherwood number decreases with increase in the angle of inclination of the magnetic field but increases with increase in the unsteadiness parameter.
- Further research may be carried out to expand the model and include a three-dimensional fluid flow for a more realistic representation of practical engineering systems.

Disclaimer (Artificial Intelligence)

Author(s) hereby declares that generative AI technologies such as Large Language Models, etc. have not been used during the writing or editing of manuscripts

Competing Interests

Authors have declared that no competing interests exist.

References

Bhatti, M., Zeeshan, A., Ijaz, N., & Ellahi, R. (2017). Heat transfer and inclined magnetic field analysis on peristaltically induced motion of small particles. *Journal of the Brazilian Society of Mechanical Sciences and Engineering*, *39*, 3259–3267.

Dar, A. A. (2021). Peristaltic motion of micropolar fluid with slip velocity in a tapered asymmetric channel in presence of inclined magnetic field and thermal radiation. *Sohag Journal of Mathematics*, *8*(1), 9–22.

Dar, A. A., & Elangovan, K. (2017). Impact of an inclined magnetic field, heat generation/absorption and radiation on the peristaltic flow of a micropolar fluid through a porous non-uniform channel with slip velocity. *New Trends in Mathematical Sciences*, *5*(3), 227–244.

Dar, A. A., & Elangovan, K. (2017). Inclined magnetic field and thermal radiation effect on electroosmotic flow of a micropolar fluid through a porous micro-channel. *Journal of Advanced Mathematics and Applications*, *6*(1), 18–29.

Elmhedy, Y., Abd-Alla, A. M., Abo-Dahab, S. M., Alharbi, F. M., & Abdelhafez, M. A. (2024). Influence of inclined magnetic field and heat transfer on the peristaltic flow of Rabinowitsch fluid model in an inclined channel. *Scientific Reports*, *14*(1), Article 4735.

Elshehabey, H. M., Hady, F., Ahmed, S. E., & Mohamed, R. (2014). Numerical investigation for natural convection of a nanofluid in an inclined L-shaped cavity in the presence of an inclined magnetic field. *International Communications in Heat and Mass Transfer*, *57*, 228–238.

Fatunmbi, E. O., Adeosun, A. T., & Okoya, S. S. (2023). Entropy generation analysis in an unsteady hydromagnetic micropolar fluid flow along an exponentially stretchable sheet with slip properties. *International Journal of Modelling and Simulation*, *43*(4), 491–506.

Krishna, M. V., Anand, P. V. S., & Chamkha, A. J. (2019). Heat and mass transfer on free convective flow of a micropolar fluid through a porous surface with inclined magnetic field and Hall effects. *Special Topics & Reviews in Porous Media: An International Journal*, *10*(3), 227–243.

Mahabaleshwar, U. S., Rudraiah, M., Huang, H., & Sunden, B. A. (2024). An impact of ternary nanofluid on a micropolar fluid with inclined MHD, slip flow and heat transfer. *International Journal of Numerical Methods for Heat & Fluid Flow*, *34*(5), 2065–2093.

Mutegi, R., Okello, J. A., & Kimathi, M. (2021). Analysis of effect of inclined magnetic field on MHD boundary layer flow over a porous exponentially stretching sheet subject to thermal radiation. *Asian Research Journal of Mathematics*, *17*(9), 20–33.

Patel, H. R., Patel, S. D., & Darji, R. (2022). Mathematical study of unsteady micropolar fluid flow due to non-linear stretched sheet in the presence of magnetic field. *International Journal of Thermofluids*, *16*, 100232.

Pop, I., Groșan, T., Revnic, C., & Roșca, A. V. (2023). Unsteady flow and heat transfer of nanofluids, hybrid nanofluids, micropolar fluids and porous media: A review. *Thermal Science and Engineering Progress*, *46*, 102248.

Raju, C., Sandeep, N., Sulochana, C., Sugunamma, V., & Babu, M. J. (2015). Radiation, inclined magnetic field and cross-diffusion effects on flow over a stretching surface. *Journal of the Nigerian Mathematical Society*, *34*(2), 169–180.

Reddy, S. R. R., & Anki Reddy, P. B. (2021). Numerical simulations of unsteady 3D MHD micropolar fluid flow over a slendering sheet. *Journal of Applied and Computational Mechanics*, *7*(3), 1403–1412.

Sadiq, M. N., Sarwar, B., Sajid, M., & Ali, N. (2022). Heat transfer in unsteady separated stagnation point flow of a micro-polar fluid: Cattaneo–Christov model. *Journal of Thermal Analysis and Calorimetry*, *147*(8), 5199–5209.

Shamshuddin, M. D., Mishra, S. R., Bég, O. A., & Kadir, A. (2019). Unsteady reactive magnetic radiative micropolar flow, heat and mass transfer from an inclined plate with Joule heating: A model for magnetic

polymer processing. *Proceedings of the Institution of Mechanical Engineers, Part C: Journal of Mechanical Engineering Science*, *233*(4), 1246–1261.

Sheikh, N., & Hasan, M. (2017). Mixed convective flow of micropolar fluids past an inclined porous flat plate. *Open Journal of Fluid Dynamics*, *7*(4), 642–656.

Shobha, K. C., & Patil, M. B. (2022). Irreversibility analysis of micropolar nanofluid flow in a vertical channel with the impact of inclined magnetic field and heat source or sink. *Heat Transfer*, *51*(3), 2723–2741.

Srinivasulu, T., & Goud, B. S. (2021). Effect of inclined magnetic field on flow, heat and mass transfer of Williamson nanofluid over a stretching sheet. *Case Studies in Thermal Engineering*, *23*, 100819.

Srivastava, N. (2014). Analysis of flow characteristics of the blood flowing through an inclined tapered porous artery with mild stenosis under the influence of an inclined magnetic field. *Journal of Biophysics*, *2014*, Article ID 713458.

Umadevi, K. B., Patil Mallikarjun, B., & Bhattacharyya, S. (2021, December). Impact of an inclined magnetic field on non-isothermal vertical surface flow of micropolar fluid embedded in porous stratum. In *Conference on Fluid Mechanics and Fluid Power* (pp. 25–30). Springer Nature Singapore.

Vijayalakshmi, P., & Sivaraj, R. (2023). Heat transfer analysis on micropolar alumina–silica–water nanofluid flow in an inclined square cavity with inclined magnetic field and radiation effect. *Journal of Thermal Analysis and Calorimetry*, *148*(2), 473–488.

Walelign, T. (2024). Rates of heat, mass and momentum transfer in a magnetic nanofluid near cylindrical surface with velocity slip and convective heat transfer. *Heliyon*, *10*(6), eXXXXXX. *(Page/article ID pending)*

Walelign, T. (2025). Analysis of Casson nanofluid transport rates near a vertical stretching sheet with dissipation and slip effects. *Frontiers in Applied Mathematics and Statistics*, *11*, 1526769.

Peer-review history:
The peer review history for this paper can be accessed here (Please copy paste the total link in your browser address bar)
https://pr.sdiarticle5.com/review-history/142217